Japanese Journal of Applied Physics
Vol. 43, No. 8A, 2004, pp. 5440–5446

Photoalignment of Ferroelectric Liquid Crystals by Azodye Layers

Eugene POZHIDAEV*, Vladimir CHIGRINOV, Danding HUANG, Andrei ZHUKOV*, Jacob HO and Hoi Sing KWOK

The Hong Kong University of Science and Technology, Clear Water Bay, Kowloon, Hong Kong P.R.C.

(Received June 13, 2003; revised April 6, 2004; accepted April 13, 2004; published August 10, 2004)

The photoinduced alignment of ferroelectric liquid crystals (FLCs) onto photochemically stable azo-dye films was studied. The alignment quality of FLC display cells depends mainly on the difference between the FLC surface energy and the aligning substrates surface energy; however, the structure and thickness of FLC layers are also important. The effect of the thickness of photoaligning azodye layer on the alignment quality and multiplex operation of passively addressed FLC display cells has been investigated. An optimal (about 3–5 nm) azo-dye layer thickness that provides both the highest multiplex operation steadiness and the best contrast ratio of the FLC display cells was found. The photoaligned FLC display cells showed the contrast ratio CR $>$ 500 : 1 at the wavelength $\lambda = 0.63\,\mu$m both in surface stabilized and deformed helix FLC electrooptical modes. [DOI: 10.1143/JJAP.43.5440]

KEYWORDS: ferroelectric liquid crystals, photoinduced alignment, display cells, multiplex operation

1. Introduction

Nowadays the common method for the liquid crystal (LC) alignment is the mechanical buffing of thin polyimide films. The impurities and electrostatic charge of polyimide aligning films and the mechanical damage produced by rubbing can be completely avoided by the photoalignment technique.[1] This photo-alignment technique looks very promising particularly for FLCs, due to their extremely high sensitivity to any nonuniformity and damage of aligning layers.[2] A homogeneous, reproducible and steady FLC alignment is very important for FLC bistable switching. The phenomenon of the bistability and multiplex mode degradation of passively addressed FLC display cells, aligned using an ordinary rubbing technique, has been already discovered many years ago.[3] To improve the FLC alignment quality various aligning surfaces, including rubbed polyimide films[4–7] and photoaligned layers,[8–13] were used. Several types of photoaligning agent for FLCs have been reported before. A hybrid between linearly photopolymerized polymers (LPPs) and liquid crystal polymer (LCP) layers[2] provides a very good alignment of a deformed helix ferroelectric (DHF) FLC, but requires a complex technological procedure. Photoanisotropic azodye films combined with polyvinylalcohol can be also used for the photoalignment of FLCs; however, they do not prevent the bistability degradation.[8] Defect-free FLC displays were also fabricated using UV-irradiated polyimide films by the double exposure method.[9] A high contrast ratio and a perfectly bistable switching were demonstrated. Murakami *et al.* fabricated a half-V-shaped photoaligned FLC display, with an electrooptic performance superior to that of the FLC display prepared by rubbing with a high switching angle at a low voltage.[10] The photoalignment technique proves to be useful also for polymer-stabilized V-shape and half-V-shaped ferroelectric displays due to a low operation voltage.[10] The normal sufficiently long UV-illumination of polyimide films was shown to promote a defect-free alignment of a surface-stabilized FLC layer due to a possible generation of a low pretilt angle of the FLC on the substrate.[11,13] Additionally, a new sulfonic azodye, called SD-1, has been recently synthesized and successfully tested for the alignment of both FLCs[12] and nematic liquid crystals.[14] One remarkable property of this azodye is the pure reorientation of molecular absorption oscillators perpendicular to UV light polarization without any photochemical transformations.[14] Thus, the high photoalignment quality of FLCs onto azo-dye SD-1 layers can be achieved.[12] In this paper, we describe a method for FLC photoalignment using SD-1 aligning layers of various thicknesses. The quality of the FLC alignment and the steadiness of bistable switching in a multiplex operation of passively addressed FLC display cells are also considered. We compare also the surface free energy values of various FLC aligning layers, such as rubbed polyimides and photoaligned azodyes. The approach proves to be appropriate for the comparative characterization of different FLC aligning surfaces.

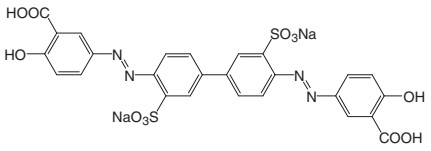

Azo-dye SD-1

2. Experimental

2.1 FLC cell preparation

Azodye SD-1 layers of various thicknesses onto ITO surfaces are obtained using N,N-dimethylformamide (DMF) solutions with different azodye concentrations from 0.2% up to 1.3%. The solutions were spin-coated onto ITO electrodes at 3500 rpm, and dried at 100°C. UV light was irradiated onto the surface of the SD-1 layer using a superhigh-pressure Hg lamp, an interference filter at 365 nm, and a polarizing filter. The light intensity on the surface of the photoaligning layer was 6 mW/cm^2 for the polarized light. The thickness of the azodye layer has been measured by the atomic force microscope (AFM). The SD-1 layer thickness was varied from 0 to 12 nm according to the concentration of SD-1 in DMF, as shown in Fig. 1.

The best FLC alignment quality has been obtained under asymmetric boundary conditions, when only one ITO

*On leave from P. N. Lebedev Physical Institute of Russian Academy of Sciences, Leninsky pr. 53, Moscow, 119924, Russia. E-mail address: epozhidaev@mail.ru

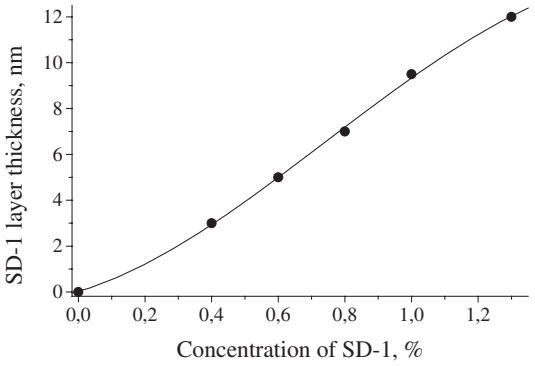

Fig. 1. Dependence of SD-1 layer thickness on SD-1 solution concentration in DMF spin-coated onto an ITO surface at 3500 rpm.

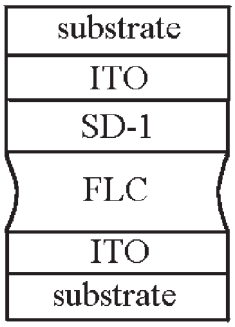

Fig. 2. Schematic drawing of an FLC cell with asymmetric boundaries. The azodye SD-1 layer was illuminated by the polarized UV light.

surface of FLC cells was prepared with the SD-1 layer, while another ITO surface was simply washed in DMF and covered with 1.5 μm or 4.85 μm diameter calibrated spacers. Thus, after assembling the FLC cells, the asymmetric boundary conditions of the FLC layer have been arranged[12] (Fig. 2). A traditional polyimide PMDA-ODA, polymeric dianhidride and 4,4′-oxydianiline layer with a uniform FLC alignment on its rubbed surface was used. After baking and imidizing the initial prepolymers, the PMDA-ODA chemical structure of reiterative links most probably corresponds to

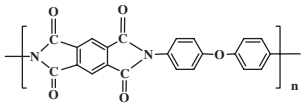

PMDA-ODA

We compared the quality of the FLC cell prepared using the rubbed polyimide layer and the photoaligned SD-1 azo-dye layer. The FLC mixtures FLC-451A, FLC-408A and FLC-445 (from P. N. Lebedev Physical Institute of Russian Academy of Sciences) have been injected into the cell in an isotropic phase by a capillary action. The physical properties of these mixtures are shown in Table I. Electrooptical measurements were carried out at $\lambda = 0.6328\,\mu m$, with the registration of electrooptical responses using an HP Infinum oscilloscope and a photodiode.

2.2 *Evaluations of surface free energy of FLC cells*

The evaluations of the surface free energy were performed using the Kaelble–Dan–Fauks method.[16] This method enables us to evaluate the free energy of low energetic surfaces through the measurements of their wetting angles Θ. The calibrated wetting liquids with known total free surface energy γ_s values, which include the polar (γ_s^P) and dispersion (γ_s^D) parts were used for the purpose. The Wendt–Owens equation[17] establishes a relationship between the unknown γ_s, γ_s^P and γ_s^D of the tested surface and the known γ_i, γ_i^P and γ_i^D of a certain calibrated wetting liquid. Here, γ_i is the total free surface energy, and γ_i^P and γ_i^D are the polar and dispersion energies correspondingly. Thus, the Wendt–Owens equation can be written as[18]

$$1 + \cos\Theta = 2(\gamma_s^D \gamma_i^D)^{1/2}/\gamma_i + 2(\gamma_s^P \gamma_i^P)^{1/2}/\gamma_i. \quad (1)$$

Equation (1) is valid under the following assumptions:

$$\gamma_s = \gamma_s^P + \gamma_s^D; \quad \gamma_i = \gamma_i^P + \gamma_i^D. \quad (2)$$

These assumptions are valid for a low-energy solid surface.[16] Equations (1) and (2) allow us to evaluate all the parameters γ_s, γ_s^P, and γ_s^D of the tested surfaces, if the parameters of the calibrated wetting liquids are known and wetting angles are measured. Let us note that for the evaluation of all parameters γ_s, γ_s^P, and γ_s^D of the tested surface it is necessary to measure contact wetting angles using at least two liquids, in order to find the solutions for eqs. (1) and (2).

We used water, glycerin and α-bromine-naphthalene as wetting liquids. Their parameters γ_i, γ_i^P and γ_i^D are known.[16] Measurements of wetting angles of tested surfaces have been carried out using the projection and interference methods developed by De Gennes.[19]

A unique finding obtained from our investigation is that wetting liquids can also wet the surface of a smectic C* ferroelectric liquid crystal. Thus, it is possible to evaluate the γ_s^D and γ_s^P values for the surface of any FLCs, if chemical interactions between the FLC and the calibrating liquid do not exist. We chose glycerin and α-bromine-naphthalene as wetting liquids for the FLC surface, because the FLC is not soluble in these liquids.

Table I. Physical properties of FLCs used in experiments.

FLC	Spontaneous polarization, nC/cm^2, at $T = 23^\circ$C	Helix pitch, μm	Phase transition
FLC-451A	150	0,27	Cr$\rightarrow^{4^\circ C}$C*$\rightarrow^{64^\circ C}$A*$\rightarrow^{87^\circ C}$Is
FLC-445	210	∞[a]	Cr$\rightarrow^{6^\circ C}$C*$\rightarrow^{78^\circ C}$A*$\rightarrow^{90^\circ C}$Is
FLC 408A	150	∞[a]	Cr$\rightarrow^{5^\circ C}$C*$\rightarrow^{54^\circ C}$A*$\rightarrow^{77^\circ C}$Is

a) The helix pitch tends to infinity as compensated in the bulk due to the interaction of the two chiral dopants with same signs of spontaneous polarization and opposite handedness.[15]

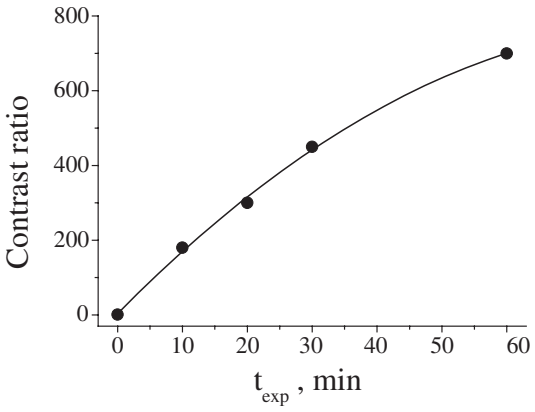

Fig. 3. Contrast ratio of FLC cells filled with the FLC-451A versus exposure time t_{exp}. The SD-1 layer was illuminated with the linearly polarized UV light ($\lambda = 365$ nm) at a normal incidence with a power density of 6 mW/cm^2. The FLC layer thickness is 4.85 μm.

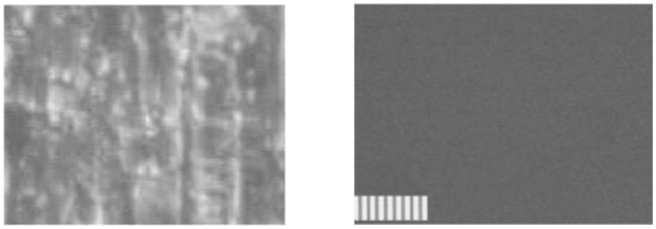

(a) (b)

Fig. 5. Polarization microscopy images of the dark state of two cells filled with the FLC-445 at different boundary conditions: (a) symmetric boundary conditions — both ITO layers of the cell are covered with 20 nm rubbed PMDA-ODA layers, (b) asymmetric boundary conditions — one ITO layer is covered with a 20 nm rubbed PMDA-ODA layer, while another ITO layer is not covered at all. The FLC layer thickness is 1.5 μm for both cells. An appendix at Fig. 8(b) illustrates a scale of both images; the striped structure of the appendix has a periodicity of 8 μm. The images were obtained immediately after the preparation of the cells; an electric field was not applied.

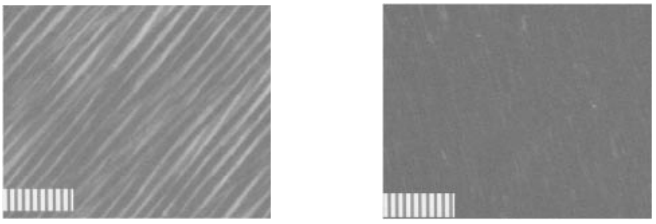

(a) (b)

Fig. 4. Polarization microscopy images of the dark state of two photoaligned cells filled with the FLC-451A, the cell gap is 1.5 μm: (a) the irradiation time of the SD-1 surface is 10 min, and (b) the irradiation time of the SD-1 surface is 60 min. The SD-1 layer thickness is 13 nm. Appendices at images illustrate the scale of the images; the striped structure of the appendices has a periodicity of 8 μm. Images were obtained immediately after the preparation of the cells; an electric field was not applied.

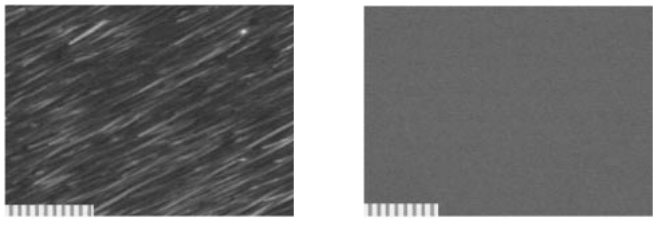

(a) (b)

Fig. 6. Polarization microscopy images of the dark state of two photoaligned cells filled with the helix-free FLC-445: (a) the irradiation time of the SD-1 surface is 10 min, (b) the irradiation time of the SD-1 surface is 60 min. The SD-1 layer thickness is 13 nm, and the FLC layer thickness is 1.5 μm. Appendices at images illustrate a scale of images; the striped structure of the appendices has a periodicity of 8 μm. The images were obtained immediately after the preparation of the cells; an electric field was not applied.

3. Results and Discussion

3.1 Dependence of FLC alignment quality on the exposure time and cell asymmetry

A sufficiently large exposure time t_{exp} (exposure energy) results in the contrast enhancement of the FLC cell up to 700 : 1 and higher due to the decrease in FLC dislocation density (Fig. 3). The images of FLC textures clearly confirm this statement (Fig. 4). The dislocation lines are visible bright stripes in the dark state [Fig. 4(a)]. The dislocations in the FLC disappear when the exposure time is sufficiently long [Fig. 4(b)].

The asymmetric boundary conditions play very important roles even if the rubbed polyimide is used instead of the azodye layer (Figs. 2 and 5). The defects can also be suppressed in this case [Fig. 5(b)]. The asymmetric preparation of FLC cell substrates was carried out to avoid a competition in the aligning action of solid surfaces. The ITO electrode itself favors a focal-conic or planar degenerated alignment, where all directions on the plane of the substrate are energetically equivalent. In contrast, the rubbed polyimide layer or the photoaligned SD-1 layer provides a preferable direction for the alignment of FLC molecules that becomes dominant in the entire FLC cell (Figs. 4 and 5).

A comparison between Figs. 4 and 5 shows that the photoaligned FLC cell could be as uniform as the FLC cell prepared by buffing, if the exposure time of the azodye photoaligning layer is sufficiently long. The helix-free FLC is more sensitive to the aligning action of the dye layer, and shows a more uniform alignment than the deformed helix FLC mixtures, *e.g.*, DHF FLC-451A (Fig. 6). The contrast ratio of a cell filled with the helix-free FLC-445 is more than 1500 : 1 for the exposure time of 60 min, and about 400 : 1 for the exposure time of 10 min. Thus, the helix-free FLC is preferable for photoalignment; as in this case, the equilibrium FLC twist is zero (compare Figs. 4 and 6).

3.2 Effect of surface free energy on FLC aligning quality

Comparative analyses of FLC cells prepared using the photoaligned azodye and rubbed polyimide can be carried out in terms of the surface free energies of the SD-1, PMDA-ODA, ITO and FLC-445 (Table II). Table II presents both the measured wetting angles with different wetting liquids and surface free energy parameters γ_s^P, γ_s^D and γ_s evaluated using eqs. (1) and (2). Note that wetting angles along (Θ_{II}) and perpendicular ($\Theta_{\perp}$) to the polarization plane of the UV-light that irradiated the SD-1 surface (or to the rubbing direction of the PMDA-ODA) are significantly different

Table II. Wetting angles and surface energies of FLC-445 surface and various aligning solid surfaces.

Surface	Measured parameters of wetting		Evaluated parameters of the surface free energy, mJ/m^2		
	H_2O, glycerin	α-bromine-naphthalene	$\gamma_{sII}{}^P$	$\gamma_{sII}{}^D$	γ_{sII}
	Θ_{II}, $\Theta_{\perp}$, deg.	Θ_{II}, $\Theta_{\perp}$, deg.	$\gamma_{s\perp}{}^P$	$\gamma_{s\perp}{}^D$	$\gamma_{s\perp}$
	64	14	8.9	43.3	52.2
Rubbed PMDA-ODA[a)]	73	28	5.9	39.6	45.5
ITO	25	75	48	18	66
SD-1, after 10 min. of	62.3	20.7	20.0	37.6	57.6
UV light irradiation[b)]	56.9	11.0	22.0	38.0	60.0
FLC-445A (in ferroelectric smectic C* phase)	70	24	2.7	41.5	44.2

a) Symbols "$_{II}$" and "$\perp$" indicate the direction of rubbing and perpendicular direction, respectively.
b) Symbols "$_{II}$" and "$\perp$" indicate the direction of the polarization plane of the light during exposure and perpendicular direction, respectively.

(Table II). We can introduce the corresponding anisotropy $\Delta\gamma_S$,

$$\Delta\gamma_S = \gamma_{SII} - \gamma_{S\perp}, \tag{3}$$

where γ_{SII} and $\gamma_{S\perp}$ are the surface free energies parallel and perpendicular to the polarization plane of the UV-light (or to the rubbing direction of the PMDA-ODA). Table II shows that $\Delta\gamma_S = 6,7\,\mathrm{mJ/m^2}$ for the rubbed surface of the PMDA-ODA, while $\Delta\gamma_S = 2,4\,\mathrm{mJ/m^2}$ for the SD-1 surface irradiated by the polarized UV-light during 10 min. The value of $\Delta\gamma_S$ depends on the exposure time of the SD-1 surface [Fig. 7(a)], and consequently, the contrast ratio increases with increasing $\Delta\gamma_S$ [Fig. 7(b)].

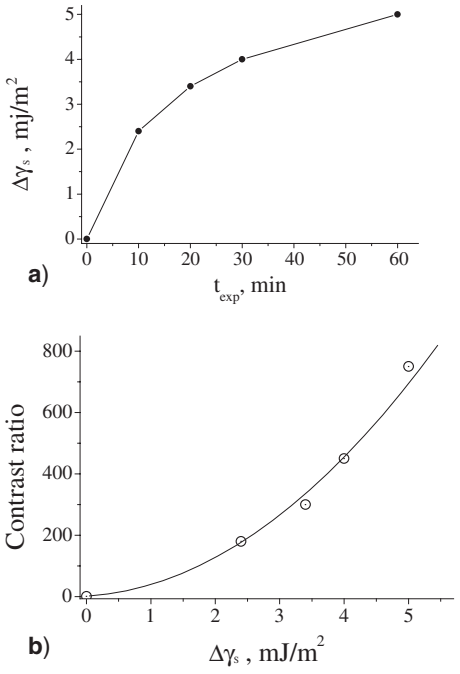

Fig. 7. (a) Dependence of the anisotropy of the SD-1 surface free energy on the exposure time t_{exp} of the SD-1 surface with the polarized UV light; (b) Dependence of the contrast ratio on the anisotropy of the SD-1 surface free energy for the case of 1.5 μm photo-aligned cells filled with the FLC-451A at an SD-1 layer thickness of 12 nm.

A homogeneous alignment of the nematic liquid crystal on the surface usually takes place when the energy of the solid surface is larger than the surface energy of the nematic liquid crystal layer.[20)] In this case, the surface tension of a solid substrate dominates over the surface tension of a liquid crystal and, therefore, the surface free energy of the interface is minimized, when the liquid crystal molecules are packed flat, i.e., aligned parallel to the substrate. However this statement has never been discussed thus far for FLCs. The difference between the surface energy of the solid substrate and the liquid crystal $\Delta\gamma_{SL}$ can be written as

$$\Delta\gamma_{SL} = \gamma_S^{\mathrm{Solid}} - \gamma_S^{\mathrm{Liquid}}. \tag{4}$$

According to eq. (4) and Table II, the difference between the FLC-445 (in ferroelectric smectic C* phase) and SD-1 surface energies measured perpendicular to the plane of the polarized light is $\Delta\gamma_\perp^{\text{SD-1}} = \gamma_{S\perp}^{\text{SD-1}} - \gamma_S^{\text{FLC-445}} = 15,8\,\mathrm{mJ/m^2}$, while in the corresponding parallel direction, $\Delta\gamma_\parallel^{\text{SD-1}} = \gamma_{S\parallel}^{\text{SD-1}} - \gamma_S^{\text{FLC-445}} = 13,4\,\mathrm{mJ/m^2}$. The relative difference in surface energy between the rubbed polyimide PMDA-ODA surface and FLC surface is $\Delta\gamma_{S\parallel}{}^{\text{PMDA-ODA}} = \gamma_{S\parallel}{}^{\text{PMDA-ODA}} - \gamma_S^{\text{FLC-445}} = 8,0\,\mathrm{mJ/m^2}$ while $\Delta\gamma_{S\perp}{}^{\text{PMDA-ODA}} = \gamma_{S\perp}^{\text{PMDA-ODA}} - \gamma_S^{\text{FLC-445}} = 1.3\,\mathrm{mJ/m^2}$. Probably, one advantage of the asymmetric photoaligned SD-1 in comparison with the asymmetric rubbed PMDA-ODA is the larger difference in surface energy (4) that usually results in the higher uniformity of FLC alignment (Fig. 6).

Under asymmetric boundary conditions with the photo-aligned azodye SD-1 and ITO surfaces, we obtain the largest possible value of the surface energy difference $\Delta\gamma_{SL} \approx 37.6\,\mathrm{mJ/m^2}$ (Table II) and the uniformity of FLC alignment is perfect (Fig. 6). Thus according to our experiments, the most important parameter that defines the quality of FLC alignment is the absolute value of the liquid crystal-solid substrate surface energy difference $\Delta\gamma_{SL}$. This value taken in the preferred alignment direction increases for the higher anisotropy of the surface energy $\Delta\gamma_S$ (3). In other words, the increases in the $\Delta\gamma_{SL}$ and $\Delta\gamma_S$ values are necessary for a high-quality FLC alignment.

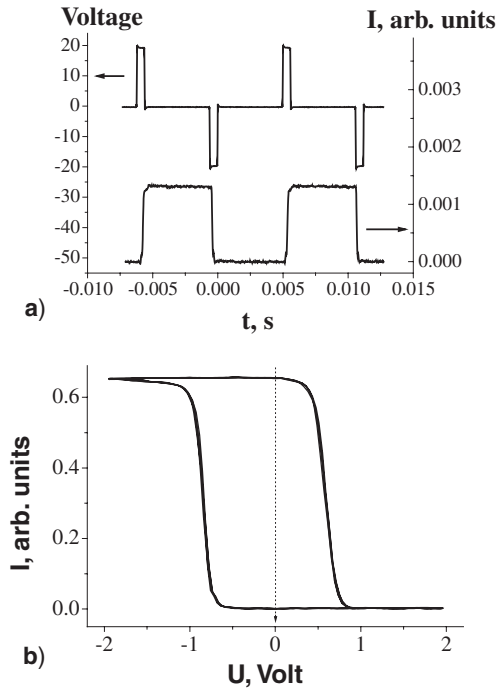

Fig. 8. Electrooptical responses of the photo-aligned asymmetric 5 μm cell filled with the helix-free FLC-445: (a) bottom curve — a shape of the electrooptical response, and top curve, a driving voltage waveform for checking the bistable mode; (b) a hysteresis loop in the electrooptical response of the cell under the action of a triangular voltage at a frequency of 10^{-2} Hz.

3.3 Bistable switching of FLC cell in multiplex regime

The FLC bistable switching is very sensitive to the asymmetry in boundary conditions. In our case, the bistability remains perfect and steady, as shown in Fig. 8(a), and we did not observe any change in the operation of the FLC cell bistable switching at least during six months. The switching asymmetry manifests only in the hysteresis loop of the electrooptical response under the action of a driving voltage at low frequency [Fig. 8(b)], which is not so important in our case.

All the FLC cells can be addressed in the multiplex regime, but the steadiness of the multiplex operation is strongly dependent on the duration and amplitude of driving voltage pulses, as well as on the thickness of aligning layers. We estimated the steadiness of a multiplex operation as the ratio of the noise N in the electrooptical response, produced by cross-talking pulses, to the electrooptical signal S generated by selecting pulses. The ratio of the selecting pulse amplitude to the cross-talking pulse amplitude was 3 : 1 (Fig. 9). Figure 9 illustrates the definition of the steadiness parameter N/S. The steadiness parameter varies to $0 \leq N/S \leq 1$ and depends on the duration of driving voltage pulses (Fig. 10). The dependence could be explained as follows. If the selecting pulse duration is too small for total FLC director switching, no signal will appear and the N/S ratio tends to be 1. On the other hand, if the duration of cross-talking pulses is sufficiently large for total FLC switching the cross-talking pulses can provide FLC switching together with the selecting pulses and $N/S = 1$ again (Fig. 10). The minimal value of the N/S ratio, which can be close to zero, corresponds to the highest multiplex mode steadiness.

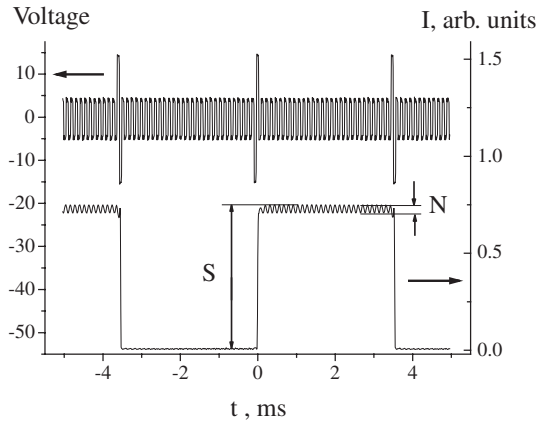

Fig. 9. Typical multiplex driving voltage shape (top curve) and electrooptical response of the FLC-408A (bottom curve) obtained with an asymmetric photo-aligned FLC cell. The cell gap is 1.5 μm, and the SD-1 layer thickness is 7 nm at $T = 25°C$. Noise (N) is the FLC electrooptical response created by cross-talking pulses, while the signal (S) is the change of the FLC response produced by selecting pulses. The ratio of the selecting pulse amplitude to the cross-talking pulse amplitude is 3 : 1.

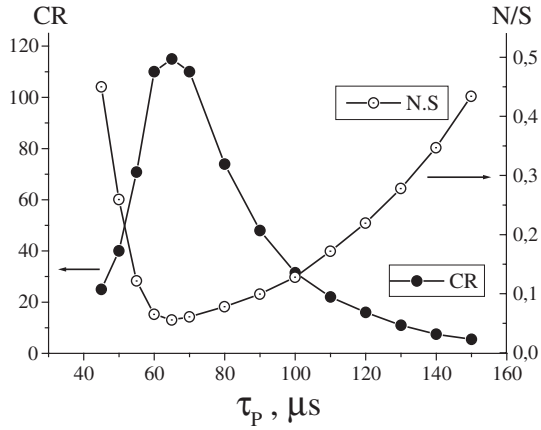

Fig. 10. Dependence of the noise to signal ratio N/S and the contrast ratio CR in the multiplex regime on the driving voltage pulses duration (the voltage has the same shape as that in Fig. 9) for a 1.5 μm FLC-408A cell; the SD-1 layer thickness is 3 nm at $T = 25°C$.

The variation in the contrast ratio of the driving voltage pulse duration $CR(\tau_P)$ has the same origin as that discussed for the noise - to signal ratio $N/S(\tau_P)$. Indeed, the noise from the cross-talking pulses in the dark state defines the contrast ratio of FLC switching. Let us also note that the contrast ratio strongly depends on FLC alignment uniformity. Usually the contrast in the statically addressed bistable mode is much higher, than that in the multiplex mode: $CR_{bis} \gg CR$ (Fig. 11).

3.4 Effect of photoaligned azodye layer thickness on FLC bistable switching

The dependence of the contrast CR_{bis} and noise-to-signal $(N/S)_{min}$ ratio on the SD-1 layer thickness $L_{DS\text{-}1}$ provides a narrow region of the SD-1 layer thickness, appropriate for the operation of passively addressed photoaligned FLC display cells. The most steady multiplex operation of passively addressed FLC display cells, as well as the highest value of the contrast ratio, is obtained, when the SD-1

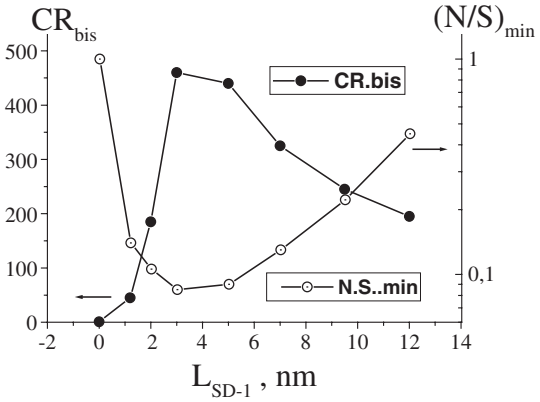

Fig. 11. Dependence of the contrast ratio CR_{bis} and the steadiness parameter $(N/S)_{min}$ of 1.5 µm FLC-445 cells in a static addressing bistable (non-multiplex) regime on the photo-aligning SD-1 layer thickness at $T = 25°C$.

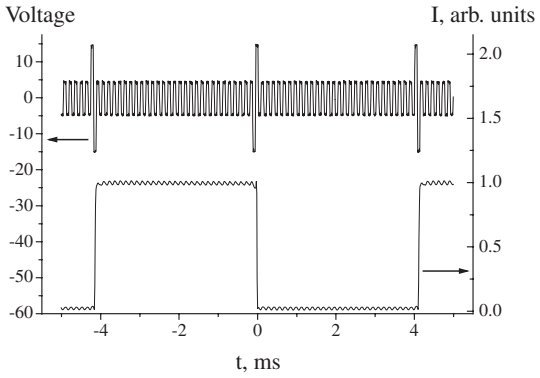

Fig. 12. Multiplex driving voltage shape (top curve) and electrooptical response of the FLC-408A cell (bottom curve). The cell gap is 1.5 µm, and the SD-1 layer thickness is 3 nm at $T = 25°C$.

azodye layer onto the ITO surface is about 3–5 nm thick (Fig. 11). The optimal SD-1 layer thickness is about 3 nm, which corresponds approximately to 5–6 monomolecular layers of SD-1 azodye molecules aligned onto the ITO surface parallel to the latter. A perfect multiplex mode occurs at optimal 3 nm aligning layer thickness exhibiting $(N/S)_{min} = 0.05$, $CR_{max} = 120:1$, while $CR_{bis} = 650:1$, all measured at the wavelength of $\lambda = 0.6328\,\mu m$ (Fig. 12). The optimal azodye photoaligning layer thickness of 3 nm corresponds to the highest uniformity of the FLC layer. The quality of FLC alignment strongly depends on the azo-dye layer thickness and a poor aligning texture with irregular focal-conic domains may appear at the thinnest SD-1 layer [Fig. 13(a)]. The domains occur due to the broken SD-1 layer, whose apparent thickness was about 1.2 nm, i.e. approximately two SD-1 monolayers are attached to the ITO surface. The SD-1 film discontinuity is not related to dust particles in this case, but it is an inherent property of the aligning film. The explosion regions of a discontinuous film are typically 10–100 µm. The texture in Fig. 13(b) illustrates the best FLC-445 alignment quality, when the thickness of the SD-1 layer is about 3 nm of a completely continuous azodye film. Only spacer defects of the texture are clearly visible here. This uniform texture is a consequence of the perfect uniformity of the azodye aligning layer.

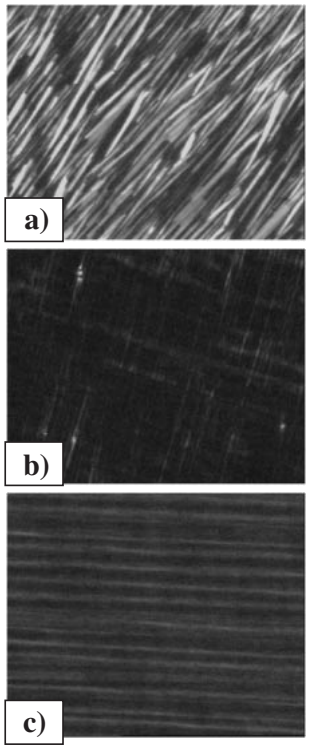

Fig. 13. Textures of 1.5 µm FLC-445 layers corresponding to different thicknesses $L_{SD\text{-}1}$ of photoaligning SD-1 layers: (a) $L_{SD\text{-}1} \cong 1.2$ nm, (b) $L_{SD\text{-}1} \cong 3$ nm, and (c) $L_{SD\text{-}1} \cong 12$ nm. The size of all is $117 \times 142\,\mu m^2$.

Increasing azodye layer thickness results in the appearance of regularly striped domains with the periodicity D along a normal to smectic layers of the FLC, as shown in Fig. 13(c). These domains are identified as ferroelectric domains in FLC cells,[21] which modulate of the FLC apparent birefringence. The FLC layers become not perfectly uniform because of the appearance of the domains. Therefore the contrast ratio decreases, and the noise parameter $(N/S)_{min}$ increases for $L_{SD\text{-}1} > 3$ nm (Fig. 11). If the SD-1 layer thickness increases further, the period of the domains becomes larger, as shown in Fig. 14, and the domains become more pronounced.

The uniform and continuous 3–5 nm photoaligning layers provide also a high spatial optical uniformity of the FLC cells over a large surface area (Fig. 15). Thus, photoaligned

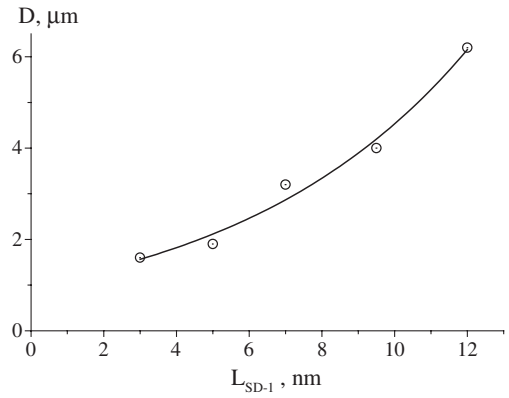

Fig. 14. Dependence of ferroelectric domain periodicity in 1.5 µm FLC-445 cells on the thickness of the photo-aligning SD-1 layer at $T = 25°C$.

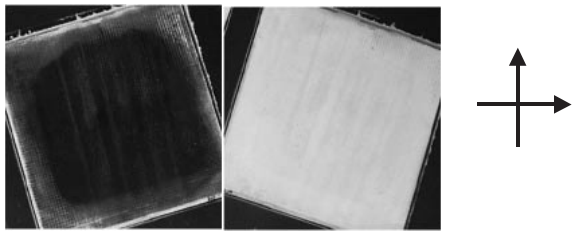

Fig. 15. FLC-408A-based 1.5 μm cell placed between two crossed polarizers, shown by arrows. The light aperture of the cell is $33 \times 33\,\mu m^2$. The dark and bright states are memorized after the driving voltage is switched off.

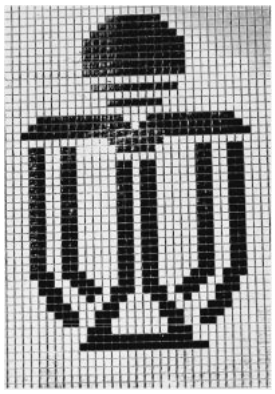

Fig. 16. Image generated by a passively addressed photo-aligned 64×64 FLC display, which is memorized after the driving voltage is switched off. The FLC-408A layer thickness is 5 μm.

FLC display cells exhibit remarkable properties that could be considered as a good scientific and technological background for the creation of passively addressed FLC bistable display devices.

A prototype of a passively addressed 64×64 display based on the photoalignment technique under asymmetric boundary conditions has been developed. The display matrix was $33 \times 33\,mm^2$ with an FLC layer thickness of 5 μm. The generation and memorizing of images during several days after switching the driving voltage have been observed (Fig. 16). We chose the 5 μm cell gap of the FLC display instead of the traditional 1.5 μm due to the higher bistable and multiplex operation steadiness and easier manufacturing of 5 μm FLC cells.

4. Conclusion

The photoinduced alignment of ferroelectric liquid crystals (FLCs) onto photochemically stable azodye films was investigated. The alignment quality of FLC display cells depends mainly on the difference between the surface energy of the aligning substrates and the FLC surface energy; however, the structure and thickness of FLC layers are also important. Asymmetric boundary conditions that provide a perfect uniformity of FLC alignment are required. The exposure energy of the SD-1 layer should be sufficiently high in this case. Another necessary condition for the uniform FLC alignment is a high anisotropy of the azodye surface free energies parallel and perpendicular to the polarization plane of the exposing UV light.

An optimal (about 3–5 nm) azodye layer thickness that provides both the highest multiplex operation steadiness and the best contrast ratio of FLC display cells was found. The optimal photoaligning layer thickness appears to be a compromise between the two types of FLC layer alignment instability: focal-conic domains and ferroelectric domains. The photo-aligned FLC display cells showed the contrast ratio $CR > 500 : 1$ at the wavelength $\lambda = 0.63\,\mu m$ in both surface stabilized and deformed helix FLC electrooptical modes. A prototype of a passively addressed 64×64 FLC display based on the photoalignment technique was developed with perfectly bistable switching in the multiplex driving regime. The FLC alignment was perfect and stable at the area of $33 \times 33\,mm^2$. The described FLC photoaligning technology could be considered as a good scientific and technological background for the creation of passively addressed bistable FLC displays.

Acknowledgements

The research was supported by RGC grant HKUST6004/01E.

1) M. Schadt, K. Schmitt, V. Kozenkov and V. Chigrinov: Jpn. J. Appl. Phys. **31** (1992) 2155.
2) J. Funfschilling, M. Stalder and M. Schadt: SID'99 Digest, 1999, p. 308.
3) Y. Inaba, K. Katagiri, H. Inoue, J. Kanbe, S. Yoshihara and S. Iijuma: Ferroelectrics **85** (1988) 255.
4) D. Williams and L. E. Davis: J. Phys. D **19** (1986) L37.
5) H. Seki, T. Uchida and Y. Masuda: Jpn. J. Appl. Phys. **26** (1987) 117.
6) H. Orihara, A. Suzuki, Y. Isyhibashi, K. Gouhara, Y. Yamada and N. Yamamoto: Jpn. J. Appl. Phys. **28** (1989) L676.
7) S. S. Bawa, A. M. Biradar, K. Saxena and S. Chandra: Appl. Phys. Lett. **57** (1990) 1398.
8) V. Vorflusev, V. Kozenkov and V. Chigrinov: Mol. Cryst. Liq. Cryst. **263** (1995) 577.
9) R. Kurihara, H. Furue, T. Takahashi and S. Kobayashi: IDW'99 Digest, 1999, p. 93.
10) Y. Murakami, J. Xu, S. Kobayashi, H. Endo and H. Fukuro: SID'02 Digest, 2002, p. 496.
11) W.-S. Kang, H.-W. Kim and J.-D. Kim: Liq. Cryst. **28** (2001) 1715.
12) E. P. Pozhidaev, V. G. Chigrinov, D. D. Huang and H. S. Kwok: Euro Display'2002 Digest, 2002, p. 137.
13) W.-S. Kang, H.-W. Kim and J.-D. Kim: Liq. Cryst. **29** (2002) 583.
14) V. Chigrinov, E. Prudnikova, V. Kozenkov, Z. Ling, H. Kwok, H. Akiyama, T. Kawara, H. Takada and H. Takatsu: Liq. Cryst. **29** (2002) 1321.
15) A. Z. Rabinovich, M. V. Loseva, N. I. Chernova, E. P. Pozhidaev, O. S. Petrashevich and J. S. Narkevich: Liq. Cryst. **6** (1989) 533.
16) A. J. Kinloch: *Adhesion and Adhesives Science and Technology* (Chapman and Hall, London, New York, 1987).
17) D. K. Owens and R. C. Wendt: J. Appl. Polym. Sci. **13** (1969) 1741.
18) R. A. Gledhill, A. J. Kinloch and S. J. Shaw: J. Adhesion **9** (1977) 81.
19) P. G. De Gennes: Rev. Mod. Phys. **57** (1985) 827.
20) T. Uchida and H. Seki: *Liquid Crystals: Applications and Uses* (World Scientific, Singapore, 1991).
21) L. A. Beresnev, M. V. Loseva, N. I. Chernova, S. G. Kononov, P. V. Adomenas and E. P. Pozhidaev: Pisma v Jurn. Eksp. Teor. Fiziki (USSR) **51** (1990) 457.